Indian Journal of Geo Marine Sciences
Vol. 49 (08), August 2020, pp. 1330-1340

Predicting wave force on vertically submerged rectangular thin plate in intermediate depth of water using second-order perturbation equation

P Deb Roy
Department of Mechanical Engineering, National Institute of Technology Silchar, Assam – 788 010, India
[E-mail: pdroy02@yahoo.co.in]

Received 27 April 2018; revised 24 September 2018

The present paper studies the nonlinearity effect of an ocean wave on a thin rectangular plate under two geometrical configurations in the intermediate water. The perturbation approximation method was derived analytically up to the second-order. Analytical results was validated by the numerical method of Simpson's 1/3 rule. Results showed that the horizontal force of the wave on a plate recorded at the water surface ($z/d = 0$) was significantly high for $\varepsilon = 0.175$ and $d/L = 0.24$ as compared to the low value of relative depth. The results also showed that the wave forces are gradually converging to each other under two types of geometrical configurations with the decrease of relative depth. Nonlinear effect of the wave forces on the plate in the form of double peaks was found in the graph at a low value of $d/L = 0.10$ and wave steepness ε (= 0.070). This study revealed that due to the effect of nonlinearity, greater wave force occurred at a depth $d = 3$ m and $T = 3$ s and $d/L = 0.24$ on a thin plate and also implied that this force does not occur at the stage of double peaks form.

[**Keywords**: Analytical result, Numerical result, Rectangular thin plate, Second-order perturbation equation, Wave force, Wave profile]

Introduction

Ocean wave is a source of renewable energy with very high energy density (energy per unit length) of the waves. The conversion of wave energy into mechanical or electrical power is a crucial factor, which can be developed by different types of wave energy converter (WEC). A thin plate which submerges vertically in the ocean water and moves by the force of ocean waves in the x-direction and absorbs energy from the ocean wave is considered. The objective of the paper is to analyze the effect of the nonlinearity of the second-order perturbation equation to determine the force on a plate under two different geometrical conditions. This analysis of the rectangular thin plate in the intermediate water forms the basis of preliminary investigation in this study.

There are many studies about the wave body interaction carried out at a different time by different authors. Hanssen & Torum[1] experimentally investigated Morison's equation to determine the breaking wave forces and moments on a tripod concrete structure.

Meylan[2] investigated the wave force on the floating thin plate using free surface Green's function and the variational equation to solve the problem. The variational equation is a simple polynomial-based function. Maiti & Sen[3] numerically studied the solitary waves in the shallow water which interact with an inclined wall using MEL method. The authors analyzed time-simulation algorithm of the waves to determine the pressures and forces on the wall. Sundaravadivelu *et al.*[4] used Linear Diffraction Theory to study the wave force and moments on the well due to regular wave.

Tsai and Jeng[5] investigated the effect of oblique incident wave forces on vertical walls using Fourier Series technique. Prabhakar & Sundar[6] numerically calculated pressure variation of a short crested wave on the walls using Fourier Series approximation method and validated their results with the experimental results obtained by Nagai[7] that showed good agreement. Fenton[8] determined the wave force on the vertical wall. Mallayachari & Sundar[9] investigated the effects of regular and random wave pressure on vertical walls, using Fourier Series approach.

There are various investigations carried out by different authors to determine the effect of breaking wave forces exerted on a submerged cylinder[10-12]. Neelamani *et al.*[13] experimentally studied the effect of the regular and random wave force on a perforated square caisson.

Deb Roy & Ghosh[14] investigated the effect of linear wave force on the vertically submerged circular thin plate in shallow water using Morison's equation. Authors mainly investigated the horizontal wave force and overturning moments on a plate. Deb Roy &

Ghosh[15] also investigated the effect of oblique incident wave force in shallow water on a thin plate. Deb Roy & Ranjan[16] theoretically investigated the effect of linear wave theory to determine the wave force on a vertically submerged rectangular thin plate in shallow water using a Fourier series approximation method.

Teo[17] theoretically studied the effect of short-crested wave pressure on a vertical wall using a fifth-order Stokes wave approximation method. Jeng[18] theoretically studied the effect of partial reflection of short-crested wave kinematics from a vertical wall at various angles using third-order stokes wave approximation method.

The past literature shows that different analytical methods were used to solve the higher-order problem and the results were validated experimentally. It was also observed that most of the researchers ignore the nonlinearity effect of higher-order approximation equation on a submerged thin rectangular plate in the intermediate water. However, in the present study, a second-order perturbation approximation theory has been used to solve the wave force on a submerged rectangular thin plate in the intermediate water under two different geometrical configurations, as shown in Figure 1. The accuracy of the presented analytical data was verified by comparing the numerical data. MATLAB code was used to obtain both analytical and numerical data.

- Type I - a surface-piercing rectangular thin plate Γ_b; and
- Type II - a bottom-standing rectangular thin plate Γ_b.

Mathematical Formulation

Consider Γ_b, a thin plate of rectangular size with dimensions l_1, l_2 and l_3 vertically submerged in the intermediate water under two geometrical configurations (Fig. 1). Here, l_1, l_2 and l_3 are the thickness, length and height of the plate in the *x, y* and *z*-direction, respectively. The length in the *y*-direction considered unity as the system is 2-dimensional and the incoming wave travels in the *x*-direction. Second-order perturbation equation was solved by MATLAB coding and the analytical results validated with the numerical results by Simpson's 1/3 rule. Here, the domain region of fluid is $-d \le z \le 0$, and $-\infty < x < +\infty$ except the plate. Following two positions of the plate in the domain is shown in Figure 1:

- Type I: x = 0, $-z_2 \le z \le 0$.
- Type II: x = 0, $-z_2 \le z \le -z_1$

Consider the flow parameters as inviscid, incompressible, and irrotational flow. Assume atmospheric pressure, P_a = 0 and the Cartesian coordinates of the system incorporated in a 2D plane *x–z*. The plane is assumed to be vertical from the water surface. The measure of the *x*-axis is the direction of waves propagation and the measure of the *z*-axis is positive upward from SWL. Assume free surface of the fluid plane is *x–y*, under equilibrium condition. The geometry of the configuration is explained in Figure 1.

Governing equation

Following are the non-dimensional parameters considered:

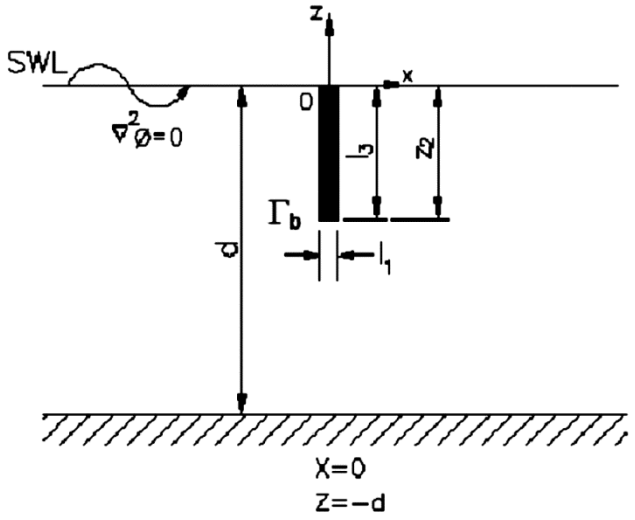

Type I A Surface–piercing rectangular thin plate

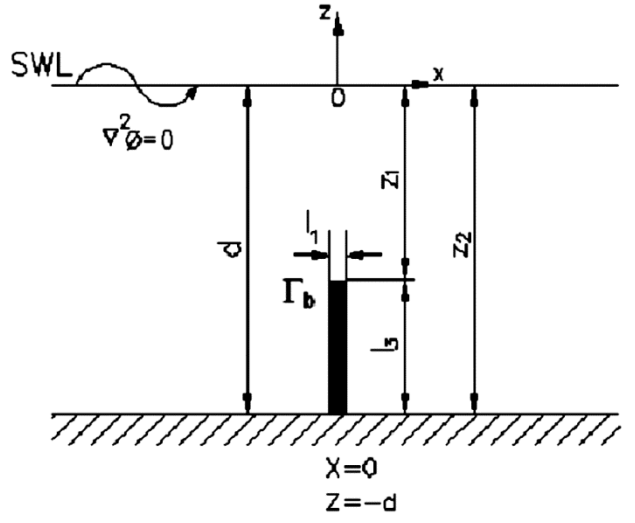

Type II A bottom standing rectangular thin plate

Fig. 1 — Definition sketch of two types of plate positions

$$\left(x^*, z^*, \eta^*, d^*\right) = k\left(x, z, \eta, d\right),\ \phi^* = \sqrt{\frac{k^3}{g}}\phi,\ t^* = \omega t,$$

$$\omega^* = \frac{\omega}{\sqrt{gk}} \quad \ldots (1a)$$

$$P^* = \frac{kP}{\rho g},\ F_x^* = \frac{F_x}{0.5\rho g d^2}, \quad \ldots (1b)$$

Where, $k=2\pi/L$ (L = wave length) and $\omega = 2\pi/T$ (T = time period), respectively. The symbol star (*) denoted the dimensionless quantities. This symbol omitted for the simplicity in sections 2 and 3.

Let, the governing equation is the Laplace equation for irrotational flow and velocity potential denoted by,

$\phi(\bar{x}, t)$.

$$\nabla^2\phi\left(\bar{x}, t\right) = 0, \quad \ldots (2)$$

Boundary conditions are:

Sets of boundary conditions required for solving the Eq. (2). The boundary conditions are:

(a) Bottom boundary condition (BBC):

$$\phi_z = 0, \text{ on } z = -d \quad \ldots (3)$$

(b) Free surface dynamic boundary condition (DFSBC):

$$\omega\phi_t + \eta + \frac{1}{2}\left(\phi_x^2 + \phi_z^2\right) = 0 \text{ on } z = 0 \quad \ldots (4)$$

(c) Free surface kinetic boundary condition (KFSBC):

$$\phi_z = \omega\eta_t + \phi_x\eta_x \text{ on } z = 0 \quad \ldots (5)$$

(d) Combined free surface boundary condition (CFSBC):

$$\phi_z + \omega^2\phi_{tt} + 2\omega\nabla\phi\cdot\left(\nabla\phi_t\right) + \nabla\phi\cdot\nabla\left(\frac{1}{2}\left(\nabla\phi\right)^2\right) = 0 \text{ on } z = 0 \quad \ldots (6)$$

Where, η is the free surface wave elevation, t time and d water depth.

Method of Solutions

Perturbation approximation

The nonlinear ordinary differential equation (ODE) solved stepwise. The first step is to convert nonlinear ODE into individual linear ODE and then solve each successively.

The velocity potential function (ϕ), and the free surface wave elevation (η) for a second-order perturbation approximation expressed in a power of wave steepness (ε):

$$\phi = \varepsilon\phi_1 + \varepsilon^2\phi_2 + \ldots, \quad \ldots (7)$$

$$\eta = \varepsilon\eta_1 + \varepsilon^2\eta_2 + \ldots, \quad \ldots (8)$$

Where, $\varepsilon\left(= ka\right)$ is a non-dimensional perturbation parameter, a is the amplitude of the waves. Subscript 1 & 2 denote quantities corresponding to the 1st order & the 2nd order perturbation solution. Substituting Eqs. (7) & (8) into the governing differential equation-2 and the boundary conditions defined by the Eqs (3) – (6), then expand through Taylor series expansion (i.e., Eq. (9)) at $z = 0$.

$$f\left(x, z; t\right) = f\left(x, 0; t\right) + \eta\frac{\partial f}{\partial z}|_{z=0} + \frac{1}{2!}\eta^2 \frac{\partial^2 f}{\partial z^2}|_{z=0} + \frac{1}{3!}\eta^3\frac{\partial^3 f}{\partial z^3}|_{z=0} + \ldots \quad \ldots (9)$$

The first-order approximation equation

The first-order problem is expressed as below:

$$\nabla^2\phi_1 = 0, \quad \ldots (10)$$

$$\omega\phi_{1t} + \eta_1 = 0, \text{ on z = 0} \quad \ldots (11)$$

$$\phi_{1z} = \omega\eta_{1t}, \text{ on z = 0} \quad \ldots (12)$$

$$\phi_{1z} + \omega^2\phi_{1tt} = 0, \text{ on z = 0} \quad \ldots (13)$$

$$\phi_{1z} = 0, \text{ on } z = -d \quad \ldots (14)$$

The first-order wave equation derived by applying the method of separate as given below:

$$\phi_1 = \frac{1}{\omega}\frac{\cosh\left(z+d\right)}{\cosh\left(d\right)}\sin\left(x-t\right), \quad \ldots (15)$$

$$\eta_1 = \cos\left(x-t\right), \quad \ldots (16)$$

$$\omega^2 = \tanh d, \quad \ldots (17)$$

The second-order approximation equation

The second-order problem is expressed as below:

$$\nabla^2\phi_2 = 0, \quad \ldots (18)$$

$$\eta_2 + \omega\phi_{2t} + \frac{1}{2}\left(\phi_{1x}^2 + \phi_{1z}^2\right) + \omega\eta_1\phi_{1zt} = 0, \text{ on } z = 0 \quad \ldots (19)$$

$$\omega\eta_{2t} - \phi_{2z} = \eta_1\phi_{1zz} - \phi_{1x}\eta_{1x} - \phi_{1z}\eta_{1z}, \text{ on } z = 0 \quad \ldots (20)$$

$$\phi_{2z} + \omega^2\phi_{2tt} = -2\omega\phi_{1x}\phi_{1xt} - 2\omega\phi_{1z}\phi_{1zt} - \eta_1\phi_{1zz} - \omega^2\eta_1\phi_{1ztt}, \text{ on } z = 0 \quad \ldots (21)$$

$$\phi_{2z} = 0, \text{ on } z = -d \quad \ldots (22)$$

Second-order velocity potential (ϕ_2) obtained by substituting Eqs. (15), (16) and (17) into the right part of the Eq. (21) as below:

$$\phi_2 = A_1 \cosh 2(z+d) \sin 2(x-t), \quad \ldots (23)$$

Second-order wave profile (η_2) obtained by introducing Eqs. (15) - (16) and (23) into Eq. (19) as below:

$$\eta_2 = B_1 \cos 2(x-t), \quad \ldots (24)$$

In Eqs. (23) and (24), the A_1 and B_1 coefficients are given as:

$$A_1 = \frac{3(\omega^{-7} - \omega)}{8\cosh 2d}, \quad \ldots (25)$$

$$B_1 = \frac{1}{4}(3\omega^{-6} - \omega^{-2}), \quad \ldots (26)$$

Pressure and force on the vertical plate

Bernoulli's equation used to determine the pressure on the plate induced by the water wave:

$$P = -z - \omega\phi_t - \frac{1}{2}[\phi_x^2 + \phi_z^2], \quad \ldots (27)$$

The integration of the above expression between the limit $-z_1$ to $-z_2$ gives the horizontal force F_x.

$$F_x = \int_{\Gamma_b} P n_x ds, \quad \ldots (28)$$

Here, ρ signified density of water. Let n_x is the normal unit vector $\bar{n}$ on Γ_b and n_x = 1 for the submerged vertical plate. Second-order difference rules used to determine the time derivative ϕ_t and velocities ϕ_x.

The projected area of the plate along the *z*-axis is minimal and consider zero because the plate is in water vertically and is very thin. Again, the vertical velocity of the wave at the bottom is zero (according to BBC), and this vertical velocity increases gradually towards the free surface of the water. This velocity on the free surface is also minimal and may neglect. Hence, the vertical force is negligible on a thin plate.

Problem definition expressed, the waves propagate along the *x*-direction and no pressure variation in the *y*-direction. Consider wave pressure exerted on a plate in the *x*-direction at a location $x = 0$ (Fig. 1).

Result and Discussion

The main objective of this study is to investigate the analysis of propagating wave force of ocean on a thin plate, using the second-order Stokes wave approximation theory under two different geometrical configurations. Estimated results are considered as the maximum of six decimal places to achieve accuracy in the intermediate water ($0.05 \le d/L \le 0.5$).

Sets of numerical results and analytical results of horizontal wave force (F_x) for the two geometry of the plate in the intermediate water ranges between $0.1 \le d/L \le 0.44$ shown in Tables 1-4. Tables 1-4 shows that

Table 1 — Comparative results of analytical values (F_x) and numerical values (F_n) at d = 3 m, l_1 = 1 mm, l_3 = 0.5 m for T = 3 s & 4 s

a/d	T = 3 s, d/L = 0.24			T = 4 s, d/L = 0.16		
	$F_x\times10^{-10}$ Analytical	$F_n\times10^{-10}$ Numerical	Error (%)	$F_x\times10^{-10}$ Analytical	$F_n\times10^{-10}$ Numerical	Error (%)
			Type I (z/d=0)			
0.033	12.86661	12.44418	3.2831	6.398245	6.191826	3.2262
0.050	19.71234	19.08092	3.2032	10.07943	9.767498	3.0947
0.067	26.81946	25.98968	3.0940	14.06272	13.65182	2.9219
0.083	34.17780	33.16714	2.9571	18.33347	17.83619	2.7124
0.100	41.77717	40.60995	2.7939	22.87685	22.31183	2.4698
0.116	49.60735	48.31478	2.6056	27.67782	27.06981	2.1968
			Type II (z/d=-1)			
0.033	5.853973	5.657958	3.3484	4.135963	3.997834	3.3397
0.050	8.744160	8.451394	3.3481	6.296391	6.086169	3.3388
0.067	11.60705	11.21850	3.3475	8.508750	8.224799	3.3372
0.083	14.44055	13.95728	3.3466	10.76555	10.40652	3.3349
0.100	17.24255	16.66574	3.3453	13.05912	12.62397	3.3322
0.116	20.01095	19.34185	3.3437	15.38161	14.86959	3.3288

Table 2 — Comparative results of analytical values (F_x) and numerical values (F_n) at d = 3 m, l_1 = 1 mm, l_3 = 0.5 m for T = 5 s & 6 s

a/d	T = 5 s, d/L = 0.12			T = 6 s, d/L = 0.10		
	$F_x\times10^{-10}$ Analytical	$F_n\times10^{-10}$ Numerical	Error (%)	$F_x\times10^{-10}$ Analytical	$F_n\times10^{-10}$ Numerical	Error (%)
			Type I (z/d=0)			
0.033	4.060804	3.930789	3.2017	2.922622	2.829267	3.1942
0.050	6.573622	6.372898	3.0535	4.855248	4.707311	3.0469
0.067	9.384743	9.115869	2.8650	7.075390	6.872682	2.8650
0.083	12.47596	12.14628	2.6425	9.561516	9.307712	2.6544
0.100	15.82846	15.45015	2.3901	12.29089	11.99357	2.4191
0.116	19.42288	19.01292	2.1107	15.23957	14.91024	2.1610
			Type II (z/d=-1)			
0.033	3.009344	2.908930	3.3368	2.323393	2.245898	3.3354
0.050	4.706918	4.549917	3.3355	3.740919	3.616190	3.3342
0.067	6.517044	6.299790	3.3336	5.307773	5.130904	3.3323
0.083	8.426956	8.146247	3.3311	7.006536	6.773231	3.3298
0.100	10.42330	10.07641	3.3280	8.818580	8.525189	3.3270
0.116	12.49214	12.07686	3.3244	10.72407	10.36764	3.3237

Table 3 — Comparative results of analytical values (F_x) and numerical values (F_n) at d = 6 m, l_1 = 1 mm, l_3 = 0.5 m for T = 3 s & 4 s

a/d	T = 3 s, d/L = 0.44			T = 4 s, d/L = *0.26*		
	$F_x\times10^{-10}$ Analytical	$F_n\times10^{-10}$ Numerical	Error (%)	$F_x\times10^{-10}$ Analytical	$F_n\times10^{-10}$ Numerical	Error (%)
			Type I (z/d=0)			
0.016	2.565854	2.480109	3.3418	0.989763	0.956883	3.3220
0.025	3.854889	3.726257	3.3369	1.498977	1.449474	3.3024
0.033	5.147882	4.976459	3.3300	2.017522	1.951442	3.2753
0.041	6.444746	6.230708	3.3211	2.545233	2.462745	3.2409
0.050	7.745395	7.488999	3.3103	3.081941	2.983340	3.1993
0.058	9.049744	8.751325	3.2975	3.627480	3.513187	3.1508
			Type II (z/d=-1)			
0.016	0.369517	0.357154	3.3457	0.382598	0.369829	3.3376
0.025	0.552721	0.534228	3.3459	0.572223	0.553123	3.3378
0.033	0.734887	0.710299	3.3457	0.760698	0.735309	3.3375
0.041	0.916015	0.885368	3.3458	0.948013	0.916368	3.3380
0.050	1.096107	1.059432	3.3459	1.134134	1.096280	3.3377
0.058	1.275175	1.232494	3.3458	1.319051	1.275022	3.3379

analytical results and the numerical results are in good agreement, and the percentage of errors is very less in each case. Table 1 and 2, shows wave forces (F_x) act on the plate is more significant for relative water depth (d/L = 0.24) concerning the lower relative water depth (d/L = 0.16, 0.12 and 0.10). Table 1 also shows that the agreement of analytical results is less than equal to 2.9571 % with the numerical results for type I (z/d = 0) at a condition a/d (= 0.083, 0.100, 0.116) and d/L (= 0.24). It is also observed that the F_x on the plate shown in Tables 3 and 4 are less comparable to the wave forces in Table 1 and 2. This analysis concludes the fact that the effect of wave force in the surge direction on the plate at d = 3m, T = 3s and d/L = 0.24 is important in engineering sciences for the future study.

Figure 2 shows the horizontal force (F_x) versus wave amplitude (a/d = 0.033 to 0.116) curve under the conditions: d/L = 0.24, 0.16, 0.12, 0.10. The horizontal force increases with the amplitude. It shows that the horizontal force (F_x) act on the plate is more significant at d/L = 0.24 compared to (d/L = 0.16, 0.12 and 0.10). It also shows that wave forces decrease from the free surface of the water to the bottom of the water for a particular value of (a/d) ratio. It is observed from Figure 2 that horizontal force for the type-I and type-II converge to each other with the decreasing value of d/L, and when d/L = 0.10, it appears nearer to each other. Observation shows that analytical and numerical results are validated to each other and are in good agreement.

Table 4 — Comparative results of analytical values (F_x) and numerical values (F_n) at d = 6 m, l_1 = 1 mm, l_3 = 0.5 m for T = 5 s & 6 s.

a/d	T = 5 s, d/L = 0.19			T = 6 s, d/L = 0.15		
	$F_x\times10^{-10}$ Analytical	$F_n\times10^{-10}$ Numerical	Error (%)	$F_x\times10^{-10}$ Analytical	$F_n\times10^{-10}$ Numerical	Error (%)
			Type I (z/d=0)			
0.016	0.531158	0.513587	3.3082	0.341462	0.330196	3.2994
0.025	0.813518	0.786876	3.2750	0.529226	0.511986	3.2575
0.033	1.106781	1.071035	3.2297	0.728017	0.704709	3.2015
0.041	1.410731	1.365965	3.1732	0.937584	0.908214	3.1325
0.050	1.725152	1.671570	3.1059	1.157679	1.122351	3.0516
0.058	2.049830	1.987752	3.0285	1.388046	1.346966	2.9596
			Type II (z/d=-1)			
0.016	0.301616	0.291556	3.3354	0.231877	0.224143	3.3352
0.025	0.453525	0.438400	3.3350	0.351841	0.340106	3.3354
0.033	0.606078	0.585861	3.3356	0.474318	0.458498	3.3353
0.041	0.759193	0.733869	3.3357	0.599171	0.579193	3.3343
0.050	0.912797	0.882351	3.3355	0.726279	0.702063	3.3343
0.058	1.066818	1.031237	3.3352	0.855502	0.826978	3.3342

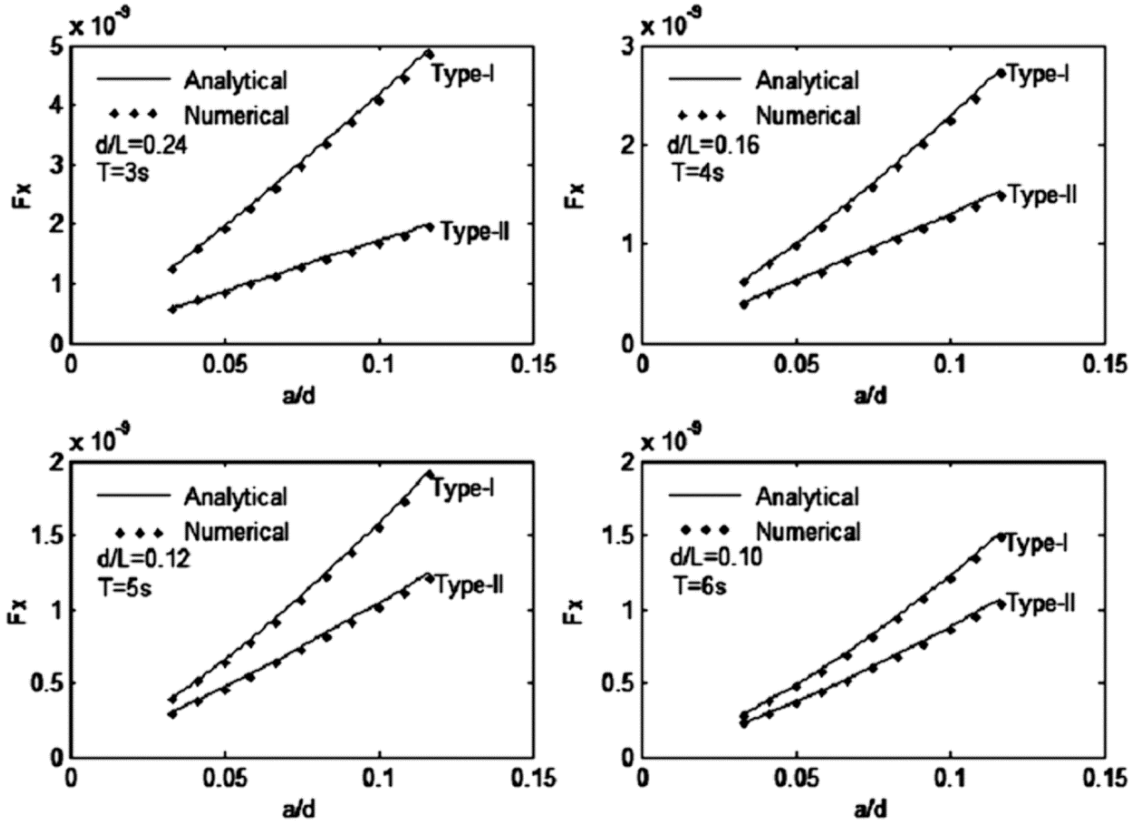

Fig. 2 — Comparison of analytical and numerical wave force (F_x) at d = 3 m, l_1 = 1 mm and l_3 = 0.5 m for the type I & type II

Horizontal force (F_x) versus wave amplitude (a/d = 0.016 to 0.058) curves are shown in Figure 3 under the various consideration of d/L = 0.44, 0.26, 0.19, 0.15. Observation shows that the effect of horizontal force (F_x) on a plate is significantly higher for d/L = 0.44 as compared to (d/L = 0.26, 0.19, 0.15). It shows that wave forces decrease from the free surface of the water to the bottom of the water for a particular value of (a/d) ratio. It is observed from Figure 3, horizontal force for the type-I and type-II are converging to each other with the decreasing value of d/L, and when d/L = 0.15, it appears very

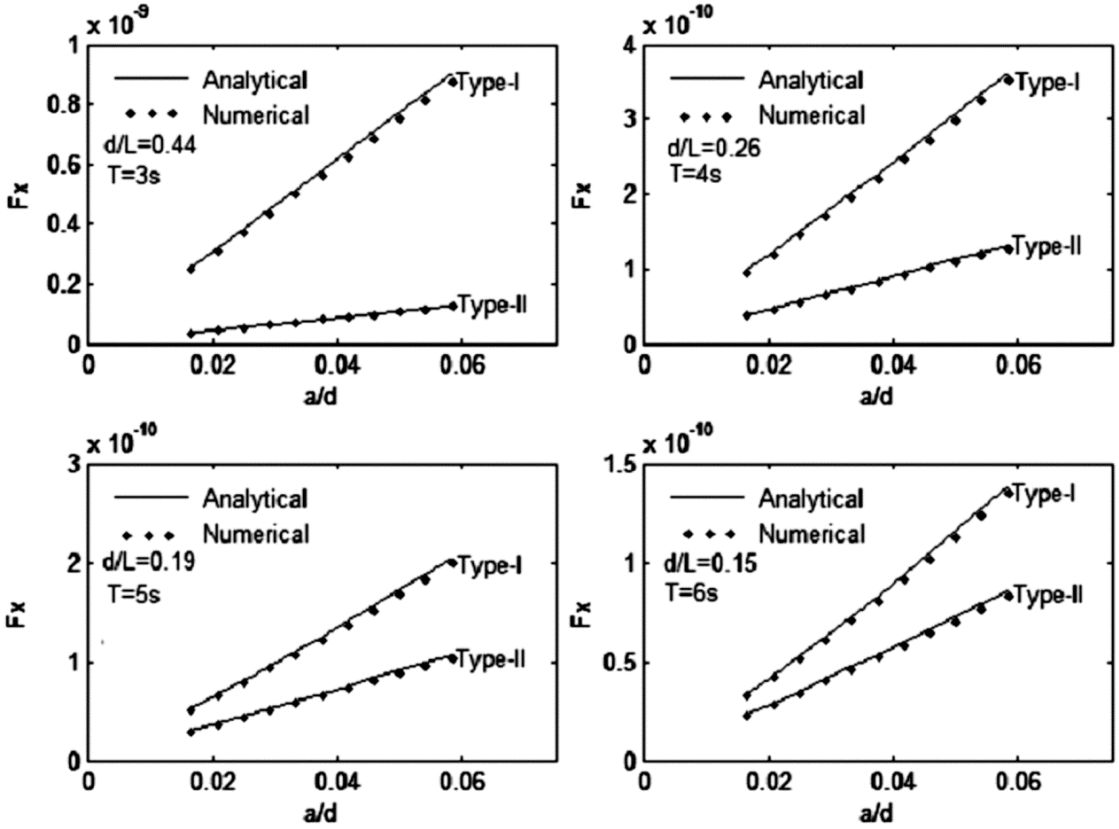

Fig. 3 — Comparison of analytical and numerical wave force (F_x) at d = 6m, l_1 = 1mm and l_3 = 0.5m for the type I & type II.

close. Here, both the analytical results and numerical results are validated to each other and showing good agreement.

Figures 2 and 3 show that surging force for the type-I and type-II close to each other at a minimal relative water depth. At a value, d/L = 0.064, the forces of the two types is almost the same (Deb Roy *et al.*[14]) indicating that the forces of the two types are nearly same. Figures 2 and 3 also show that at a depth d = 3 m and d/L = 0.24, the horizontal force acting on a plate at z/d = 0 is significantly high when compared to the value at d = 6 m and (d/L = 0.44). This explanation concludes that the effect of wave body interaction at a value d/L = 0.24 takes an essential role for further study in engineering sciences.

Time histories of horizontal forces (F_x) plotted under the different value of wave steepness (ε) at a depth d = 3 m is shown in Figure 4. Hear, relative depths consider d/L= 0.24, 0.16, 0.12, 0.10. Here, explaining the effects of propagating wave force on a plate at z/d = 0 using the second-order Stokes wave equation is an important study of the nonlinearity. Nonlinearity effect in the form of a double peak is evident in the time history of the wave forces and its effect at d/L = 0.10 on the plate shown in Figure 4 is high. Observation from figures tells that double peak found for the wave steepness ε (= 0.070) and at d/L = 0.10 between the time ranges $0.33 \le t/T \le 0.65$ implies maximum force on the plate does not always occur in this range. This research concludes to a useful guide to the design of thin vertical plate in the intermediate water depth.

Time histories of horizontal forces (F_x) plotted at the bottom position of the plate (z/d = -1) at d = 3 m shown in Figure 5 under the same conditions as the previous figures. Here, the double peak found between the time ranges $0.35 \le t/T \le 0.63$, which shows that the high nonlinearity effect extends to the bottom also.

The observation of Figure 6 shows the time histories graph of horizontal forces (F_x) on a plate at d = 6 m. Here, the position of the plate at the surface of water (z/d = 0), and d/L = 0.44, 0.26, 0.19, 0.15 under various wave steepness (ε) conditions. Here, the nonlinearity effects on the plate are not evident at all the values of d/L.

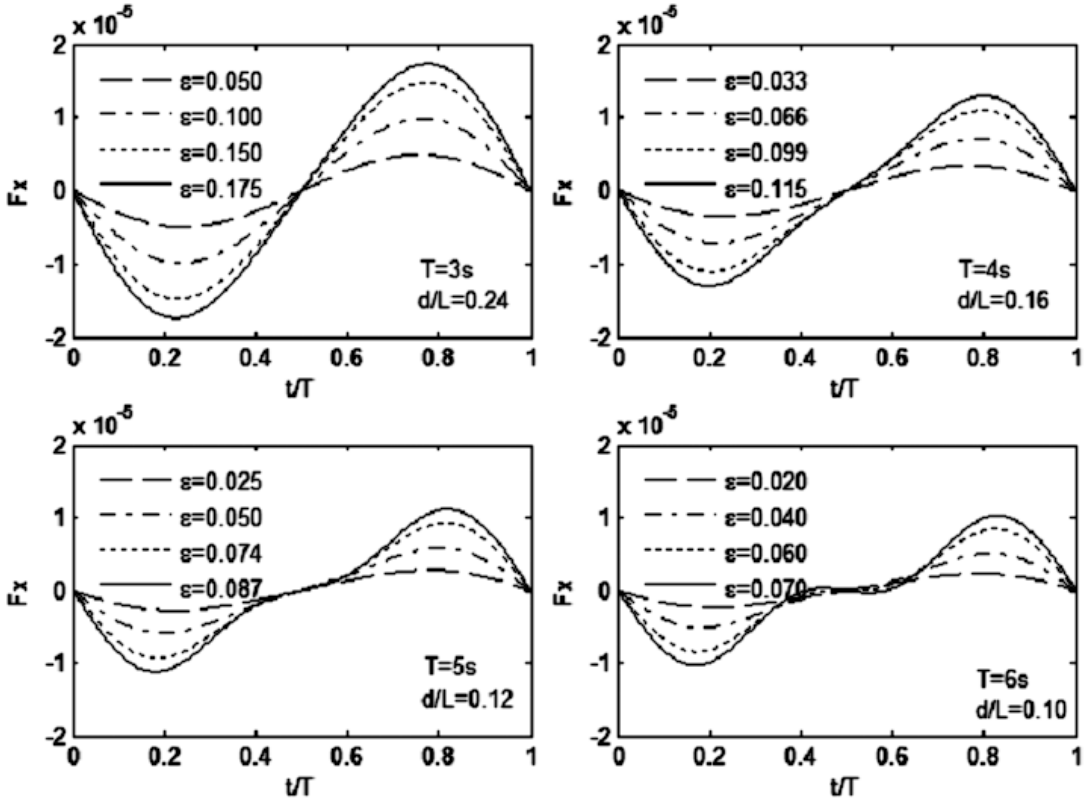

Fig. 4 — Time history of horizontal force (F_x) at d = 3 m for the type I

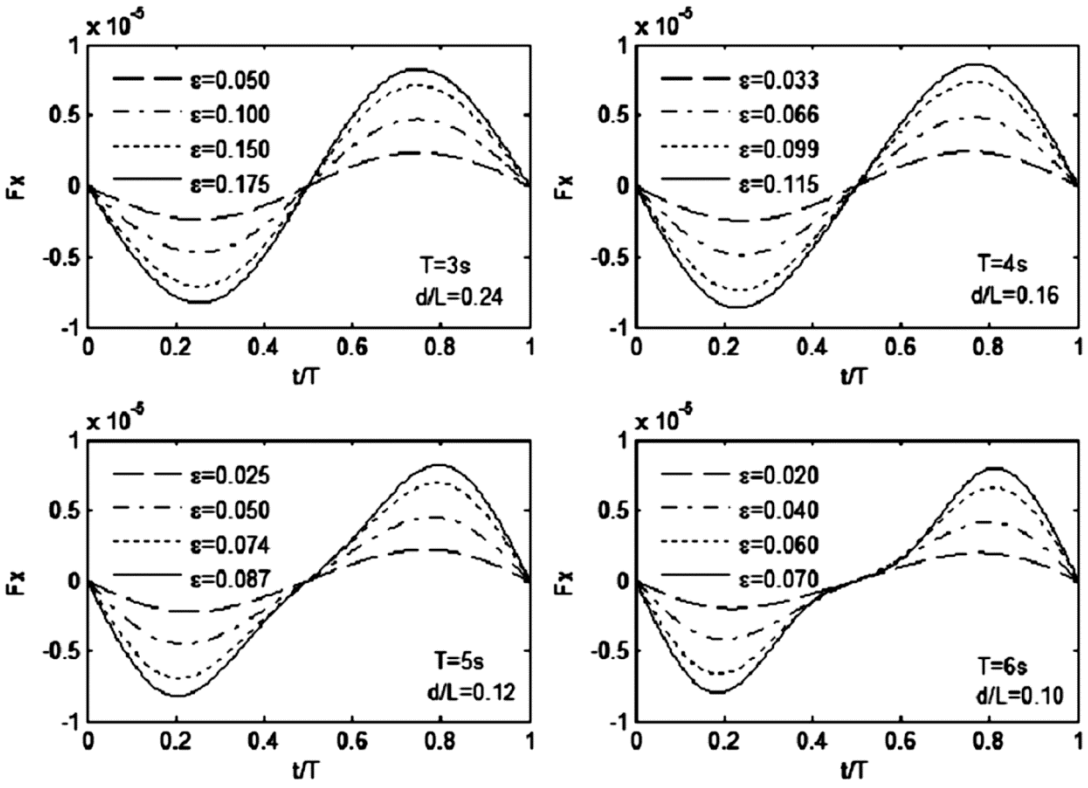

Fig. 5 — Time history of horizontal force (F_x) at d = 3 m for the type II

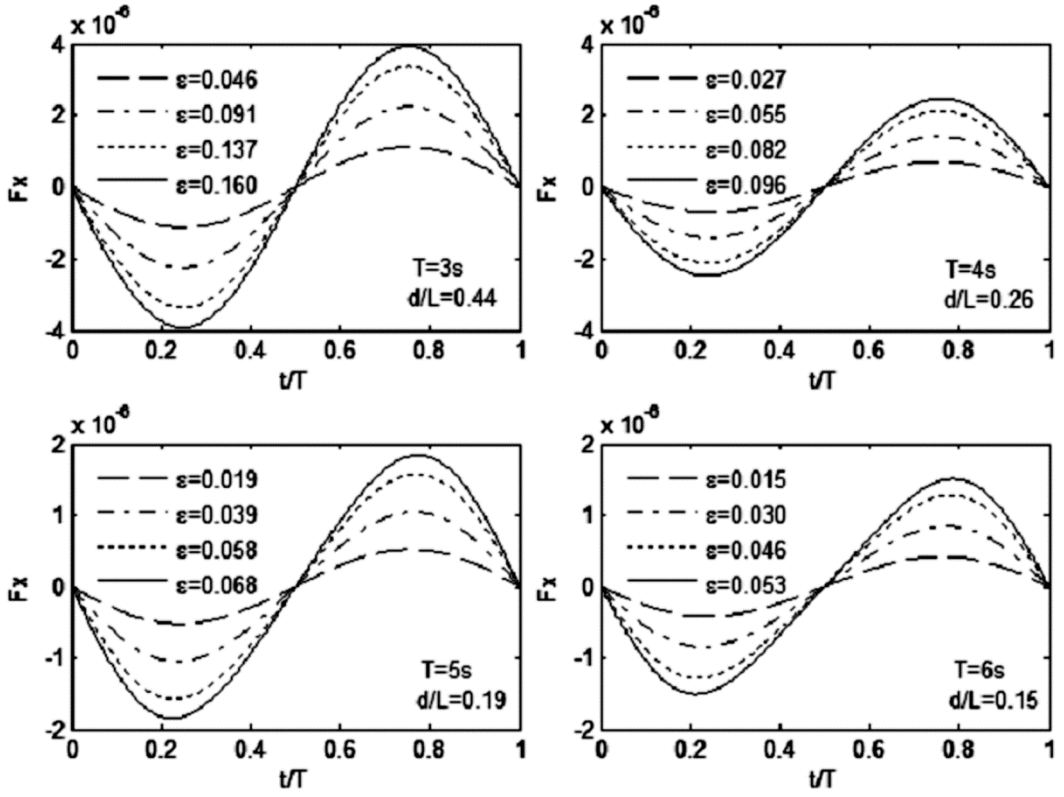

Fig. 6 — Time history of horizontal force (F_x) at d = 6 m for the type I

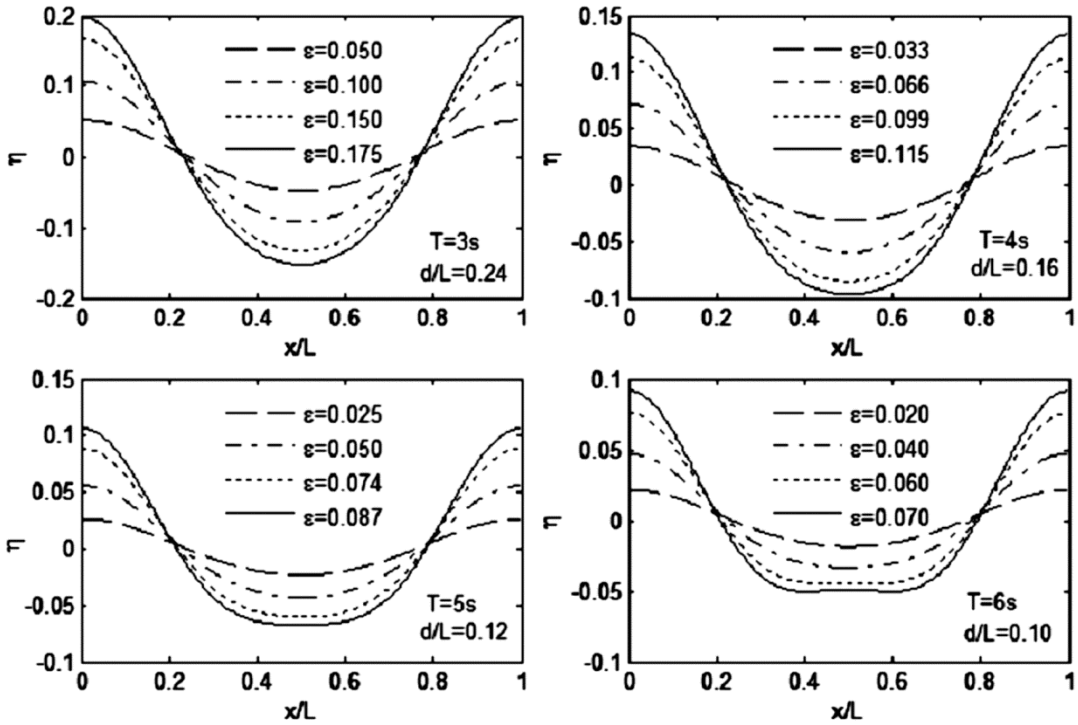

Fig. 7 — Wave profiles (η) versus (x/L) for different values of (ε) and (d/L) at d = 3 m

Figures 7 and 8 illustrate the distribution of wave profiles (η) in the x-direction under the various wave steepness (ε) conditions and various values of relative depth (d/L). The results presented in figures

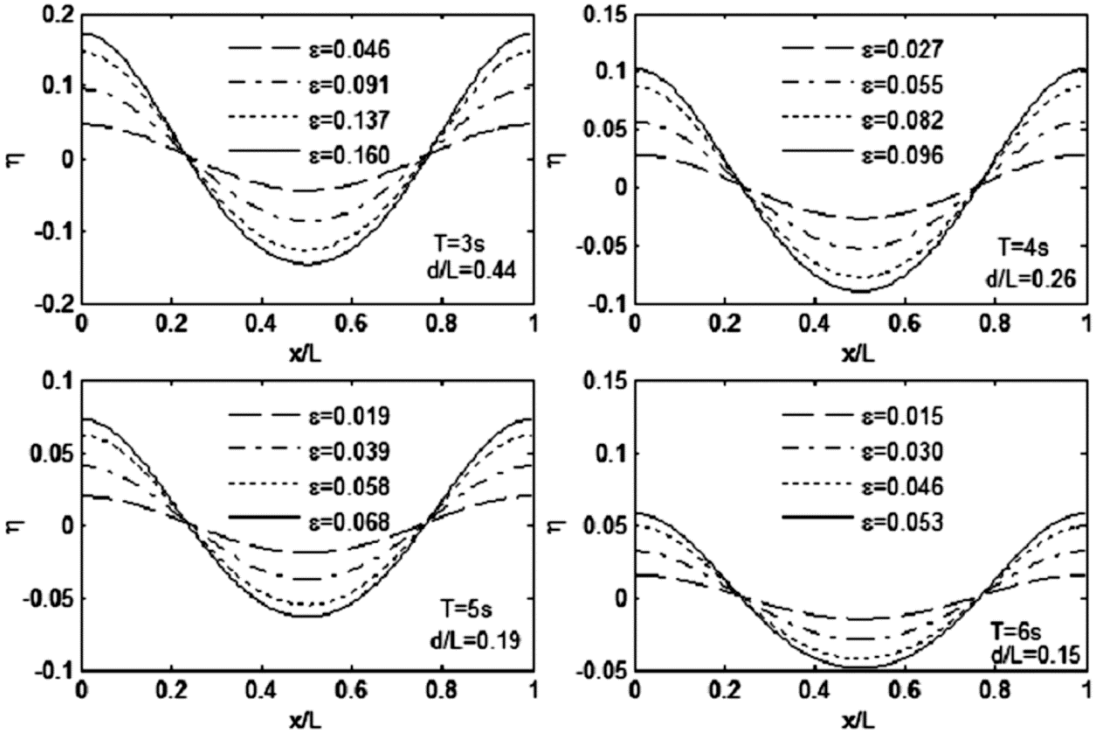

Fig. 8 — Wave profiles (η) versus (x/L) for different values of (ε) and (d/L) at d = 6 m

calculated from the second-order approximation method. It is observed from Figure 7 that steeper crest found at d/L = 0.24 and wave steepness (ε = 0.175). The value of the steeper crest gradually decreases with the decrease of relative depth. The observation of Figure 7 shows that the flatter trough with a double peak found at d/L = 0.10 and wave steepness (ε = 0.070). This observation implies that the nonlinearity effect is more potent than in a small wave steepness (ε = 0.020) under the same condition of d/L = 0.10. This indication is an important observation that the higher-order solution is essential. It also observed from Figure 8 that small flatter trough found at d/L = 0.15 and wave steepness (ε = 0.053).

Conclusion

In this analysis, the second-order Stokes wave approximation equation was used to determine the horizontal wave force on a thin rectangular plate under the condition at the surface piercing position and bottom standing position. The analysis completed at the intermediate range ($0.1 \le d/L \le 0.44$). The above approximation equation demonstrates the effect of the nonlinearity of the higher-order components of the wave forces and wave profiles on a plate. Nonlinearity effect of wave force on a plate found in the form of double peaks is the critical study. Observation of figures tells that double peak found at the wave steepness ε (= 0.070) and at d/L = 0.10 between the time ranges $0.33 \le t/T \le 0.65$, which implies maximum force on the plate does not always occur in this range. Hence, it is concluded that at a low relative depth, nonlinearity effect of the wave can be taken into consideration for further study. Observation also shows that at the mean water level (z/d = 0), the effect of wave force on the plate significantly high for d/L = 0.24 and at ε = 0.175 as compared to the low value of d/L. This analysis of the research helps the guidance to the designer who makes the design of WEC and tries to extract the energy from the ocean wave with the help of thin vertical plate in the intermediate water in the surge direction.

References

1 Hanssen A G & Torum A, Breaking wave forces on tripod concrete structure on shoal, *J WaterW Port Coast*, 125 (6) (1999) 304–310.

2 Meylan M H, A variational equation for the wave forcing of floating thin plates, *Appl Ocean Res*, 23 (2001) 195–206.

3 Maiti S & Sen D, Computation of solitary waves during propagation and runup on a slope, *Ocean Eng*, 26 (11) (1999) 1063–1083.

4 Sundaravadivelu R, Sundar V & Rao T S, Technical note: wave forces and moments on an intake well. *Ocean Eng*, 26 (1997) 363–380.

5 Tsai C P & Jeng D S, Forces on vertical walls due to obliquely incident waves, In: *Coastal Engineering*, (Elsevier, Amsterdam, Netherlands), 1990, pp. 1742-1754.
6 Prabhakar V & Sundar V, Standing wave pressures on walls, *Ocean Eng*, 28 (5) (2001) 439–455.
7 Nagai S, Pressure of standing waves on vertical wall, *J Water W Harbors Div*, 95 (1) (1969) 53–76.
8 Fenton J D, Wave force on vertical walls, *J Water W Port Coast Ocean Eng*, *ASCE*, 111 (4) (1985) 693–719.
9 Mallayachari V & Sundar V, Pressure exerted on vertical walls due to regular and random waves, In: *Proceedings of the International Symposium: Waves-Physical and Numerical Modeling*, August 1994, pp. 21–24.
10 Sawaragi T & Nochino M, Impact forces of nearly breaking waves on a vertical circular cylinder, *Coast Eng Japan*, *Tokyo*, 27 (1) (1984) 249-263.
11 Apelt C J & Piorewiez J, Laboratory studies of breaking wave forces acting on vertical cylinders in shallow water, *Coast Eng*, 11 (3) (1987) 241–262.
12 Hovden S I & Torum A, Wave forces on vertical cylinder on a reef. In: *Proceedings of the Third International Conference on Port Coastal Engineering for Developing Countries*, 1991.
13 Neelamani S, Bhaskar N V & Vijayalokshmi K, Technical note: wave force on a seawater intake caisson, *Ocean Eng*, 29 (10) (2002) 1247–1263.
14 Deb Roy P & Ghosh S, Wave force on vertically submerged circular thin plate in shallow water, *Ocean Eng*, 33 (14) (2006) 1935–1953.
15 Deb Roy P & Ghosh S, Force on vertically submerged circular thin plate in shallow water due to oblique wave, *Indian J Geo-Mar Sci*, 38 (4) (2009) 411-417
16 Deb Roy P & Ranjan R, Variation of wave force on submerged object at shallow water: Fourier series technique, *Aquat Proc*, *Elsevier*, 4 (2015) 95–102.
17 Teo H T, Technical note: wave pressure on a vertical wall due to short-crested waves: fifth-order approximation, *Ocean Eng*, 30 (16) (2003) 2157–2166.
18 Jeng D S, Technical note: wave kinematics of partial reflection from a vertical wall, *Ocean Eng*, 29 (13) (2002) 1711–1724.